

Biomechanical Evaluation of a Novel Chambered Overlay Design in Endodontically Treated Mandibular Molars

Hozan S. Salhi⁽¹⁾, Jawad M. Mikaeel⁽¹⁾

ABSTRACT

Background and objectives: Endodontically treated teeth (ETT) are structurally weakened because of extensive loss of internal dentin architecture. Although adhesive overlays have been introduced as a conservative restorative approach, limited evidence exists regarding the influence of internal design modifications on fracture resistance. This study evaluated the effect of a novel biomimetic overlay design, termed the Embedded Chamber Overlay (ECO), also known as Hozan's Chambered Overlay, on the fracture resistance of lithium disilicate restorations in endodontically treated mandibular first molars.

Methods: Sixteen extracted human mandibular first molars underwent endodontic treatment and decoronation at the cemento-enamel junction level. Specimens were randomly allocated into two groups (n = 8) according to overlay design: conventional lithium disilicate overlays or ECO lithium disilicate overlays. All restorations were fabricated and adhesively cemented using standardized protocols. Fracture resistance was evaluated under axial compressive loading using a universal testing machine. Failure modes were assessed under magnification. Data were analyzed using independent samples t-tests with statistical significance set at $\alpha = 0.05$.

Results: The ECO lithium disilicate overlay group demonstrated significantly higher fracture resistance (3971 ± 20 N) than the conventional overlay group (2641 ± 20 N) ($p < 0.001$). Cohen's d analysis revealed an extremely large effect size ($d = 66.1$). All specimens exhibited catastrophic Class IV fractures involving root-level structural separation.

Conclusion: Within the limitations of this in vitro study, ECO significantly enhanced the fracture resistance of lithium disilicate restorations in endodontically treated mandibular molars, suggesting improved biomechanical performance in structurally compromised posterior teeth.

Keywords: Overlay, Biomimetic design, Lithium Disilicate, Adhesive Restoration, Hozan's Chambered Overlay

Article Information

Submission Date: 23/7/2025
Revision date: 11/8/2025
Acceptance date: 27/8/2025
Publishing date: June 2026

Affiliation Info

⁽¹⁾College of Dentistry, Hawler Medical University, Kurdistan Region, Iraq.
Corresponding Author: Hozan S. Salhi
Email: hozan.salhi@den.hmu.edu.krd
ORCID ID: <https://orcid.org/0009-0009-6234-7900>

INTRODUCTION

Endodontically treated teeth (ETT) exhibit a significantly increased risk of biomechanical failure due to the considerable loss of internal tooth structure caused by caries, endodontic access, and instrumentation.¹ Restoration of these teeth must therefore not only reinstate function but also reinforce weakened structural integrity.^{2,3} Conventional restorative strategies, such as metal post placement, have been employed to enhance the retention of full-coverage crowns; however, these are associated with complications including root perforation and vertical root fracture.^{4,5} Fiber-reinforced posts, which exhibit an elastic modulus comparable to that of natural dentin, offer more favorable biomechanical behavior by reducing stress concentrations within the root.⁶ However, establishing a sufficient ferrule frequently requires crown-lengthening procedures, which may result in an unfavorable crown-to-root ratio and a compromised long-term prognosis.⁷ Considering these limitations, restorative dentistry has increasingly shifted toward minimally invasive approaches that prioritize structural preservation. Occlusal overlays and other adhesive restorations have become particularly appealing for endodontically treated posterior teeth. These restorations often involve supragingival margins on peripheral enamel, allowing for superior adhesive bonding and easier clinical management.⁸ Finite element analysis (FEA) studies have demonstrated that when more residual tooth structure is preserved, stress tends to concentrate within the restoration rather than at the adhesive interface, reducing the risk of adhesive failure and improving overall fracture resistance.⁹ The mechanical behavior of dental restorations is strongly influenced by the choice of restorative material. Composite resins are favored for their ease of use and aesthetic benefits but may lack the mechanical strength required in high-load areas.¹⁰ Ceramics provide excellent durability and optical properties but demand more extensive preparation and are technique-sensitive.¹¹ Metallic restorations, although highly durable, often fall short in aesthetics. Amalgam, while durable and cost-effective, has declined in use due to esthetic and environmental concerns.¹² Recently, indirect composite overlays have emerged as a promising alternative, providing an elastic modulus more closely aligned with that of natural dentin and potentially enhanced

shock-absorbing capabilities under occlusal loading.¹³ These materials, due to their compliance and mechanical compatibility, may reduce internal stress accumulation and better mimic the natural cushioning effect of tooth structure. Furthermore, other biomimetic restorative materials have demonstrated improved stress distribution and more uniform deformation behavior under load compared to conventional brittle ceramics.¹⁴ These materials are particularly suited for restoring structurally compromised endodontically treated teeth. A notable innovation in adhesive restorative techniques is the endocrown, introduced by Pissis in 1995 and later developed by Bindl and Mörmann in 1999.^{15,16} This technique consolidates the core and crown into a monolithic structure that gains macromechanical retention from the pulp chamber and micromechanical retention through adhesive bonding. Endocrowns are especially beneficial for molars with severe coronal loss, where conventional post-core strategies are contraindicated due to limited remaining tooth height.¹⁷ The broader shift toward adhesive, digitally fabricated, and minimally invasive restorations is further propelled by the integration of CAD/CAM technologies, which enable precise, chairside design and manufacturing of indirect restorations. This digital workflow enhances accuracy, fit, and consistency while reducing clinical time and operator variability.^{18,19} Within this evolving landscape, the present study introduces the Embedded Chamber Overlay (ECO. This design incorporates an internal chamber within the restoration and aims to optimize stress distribution and improve fracture resistance in endodontically treated mandibular molars.

METHODS

This *in vitro* experimental study was conducted on sixteen freshly extracted human mandibular first molars, obtained following ethical approval from the Hawler Medical University Research Ethics Committee (HMUD,2425108). The teeth were extracted for prosthodontic or periodontal reasons and selected according to standardized inclusion and exclusion criteria. Teeth with caries or exhibiting only mild enamel/dentin involvement without compromising the cemento-enamel junction (CEJ) were included. Soft tissue remnants were removed using a No.¹⁵ blade and an ultrasonic scaler (UDS-K, Guilin Woodpecker

Medical Instrument Co. Ltd., Guangxi, China). All samples were examined under $\times 20$ magnification using a stereomicroscope (Labomed Magna, USA) under proper illumination to exclude any with cracks or defects. The selected teeth were disinfected and stored in 0.5% chloramine T solution (Sigma-Aldrich, Germany) at 4°C for a maximum of one month before testing to prevent dehydration and contamination. To standardize the coronal substrate and minimize anatomical variability, all specimens were horizontally sectioned at the cemento-enamel junction (CEJ) using a low-speed, double-faced diamond disc under continuous water irrigation, as illustrated in Figure 1. Each tooth was secured in a custom-fabricated acrylic jig to achieve a precise, perpendicular section relative to its long axis. The exposed dentin surface was subsequently polished with 600-grit silicon carbide abrasive paper (3M, USA) under water cooling to produce a consistent smear layer and ensure uniformity across all samples.

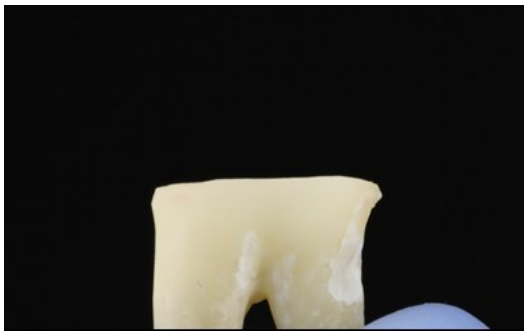


Figure 1. Sectioned sample at the CEJ

Endodontic access and sealing: Standardized endodontic access was created using a round diamond bur (Komet, Germany) followed by ProTaper rotary instrumentation (Dentsply Sirona, USA) up to F3. Canals were irrigated with 5.25% sodium hypochlorite and saline for one minute, then obturated using gutta-percha (Meta Biomed, Korea) and AH Plus sealer (Dentsply Maillefer, Switzerland) with the cold lateral condensation technique. Experimental Grouping: Sixteen teeth were randomly allocated into two experimental groups, with eight specimens assigned to each group ($n = 8$) based on overlay design: conventional lithium disilicate overlays or biomimetic chambered lithium disilicate, as shown in Table 1.

Table 1. Distribution of Experimental Groups According to Lithium Disilicate Overlay Design

Group	Design Type	Restorative Material
G1	Conventional	IPS E.max Press (Ivoclar)
G2	ECO	IPS E.max Press (Ivoclar)

Embedded Chambered Overlay Preparation: For the ECO group (G2), tooth preparation was conducted to create an internal sealed cavity simulating the natural pulp chamber. Initially, each sectioned tooth was air-abraded using 50 μm aluminum oxide particles at 2 bar pressure in a chairside sandblasting unit (MicroBlaster, Bio-Art, Brazil) to remove residual debris and smear layer. Following sandblasting, the dentin surfaces were thoroughly rinsed and cleaned with 99% ethanol (Sigma-Aldrich, Germany) to promote surface energy and improve bonding potential as shown in Figure 2.



Figure 2. Sample preparation after RCT and sandblasting

The root canal orifices were then sealed with self-adhesive flowable composite (Vertise Flow, Kerr, USA), applied directly into the canal entrances and light-cured using a 3M Elipar DeepCure-S LED curing unit (3M ESPE, USA) for 20 seconds as shown in Figure 3. This step was essential to prevent contamination by residual sealer and to maintain an internal bonding environment. A two-step self-etch adhesive system (Clearfil SE Bond, Kuraray Noritake, Japan) was applied to all exposed dentin surfaces. The primer was actively applied in two consecutive layers to maximize monomer infiltration, followed by air-drying and uniform application of the bonding resin, which was light-cured for 20 seconds. To preserve the

internal air chamber during composite reconstruction, PTFE tape (Teflon) was gently packed into

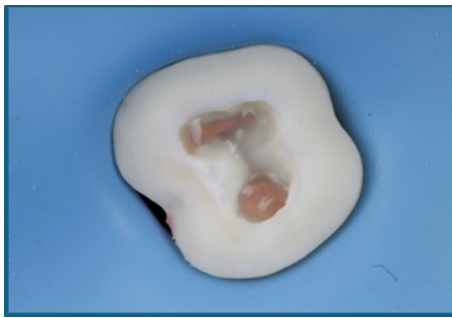


Figure 3. Sealing of root canal orifices with

This temporary barrier prevented flowable or heated composite from entering the chamber space during wall buildup. The proximal (mesial and distal), buccal, and lingual walls were then reconstructed using preheated Tokuyama Palfique LX5 composite (Tokuyama Dental, Japan) (Figure 5.) applied via a composite heater (Calset, AdDent Inc., USA) at 55°C. Composite was added incrementally and sculpted using anatomical composite instruments to replicate natural contours. Each incremental layer was polymerized using a light-curing unit for a duration of 20 seconds. After re-



Figure 5. Rebuilding proximal walls

the pulp chamber using a plastic filling instrument as shown in Figure 4.

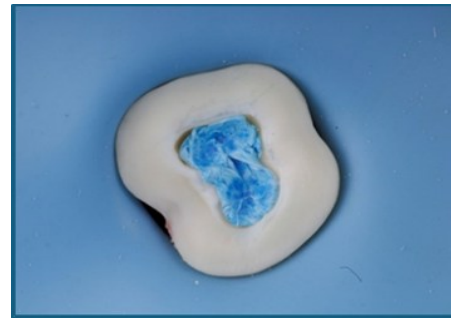


Figure 4. Application of PTFE tape as chamber barrier

moval of the Teflon barrier, all composite wall thicknesses were standardized to 1 mm using a periodontal probe to ensure uniformity across all samples as shown in Figure 6. The prepared cavity was cleaned with GC Modeling Liquid (GC Corporation, Japan) to remove surface residue and enhance the final composite adaptation. The pulp chamber ceiling was reconstructed using low-flow composite (Tokuyama Palfique LX5), carefully connecting all four internal walls (mesial, distal, buccal, and lingual) as shown in Figure 7 and 8 respectively.

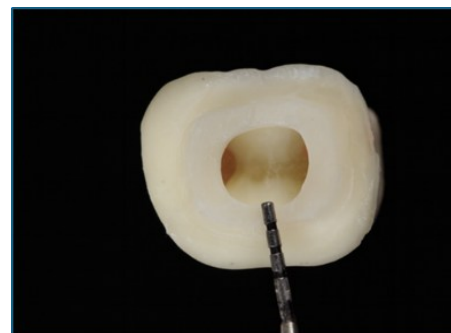


Figure 6. Standardization of internal wall thickness to 1 mm



Figure 7. Connection of mesial, distal, buccal



Figure 8. Continuation of ceiling construction and lingual walls

This formed a sealed chamber and prevented any unintentional extrusion or voids as confirmed by Bitewing X-ray (Figure 9). The composite ceiling was light-cured for 20 seconds under an oxygen inhibiting gel (DeOx, Ultradent, USA) to prevent formation of an oxygen-inhibited layer and ensure complete surface polymerization. Subsequent anatomic preparation was performed using a round-end tapered diamond bur (Komet 6847KR, Germany) to replicate the natural occlusal morphology of mandibular first molars. Special attention was given to maintain the center of the composite ceiling at the CEJ level,²⁰ while adjusting the mesial and distal wall heights to a uniform 1 mm as shown in Figure 10, providing consistent internal support for the overlay. A minimum distance of 1.5 mm was maintained between the internal walls of the embedded chamber and the external finishing line, ensuring sufficient restorative material thickness to enhance structural integrity and resist occlusal stresses as shown in Figure 11. Finally, the external finishing line was prepared as a butt-joint margin located in peripheral enamel.

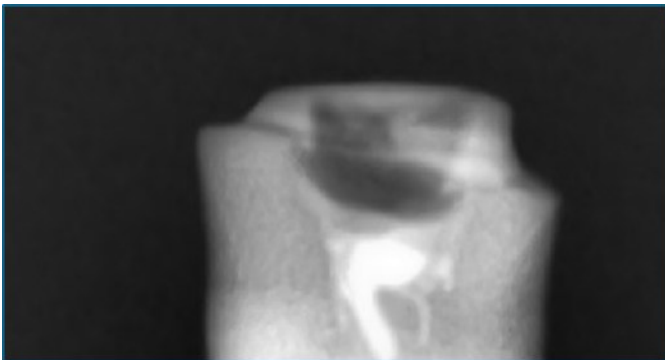


Figure 9. Formation of a sealed chamber

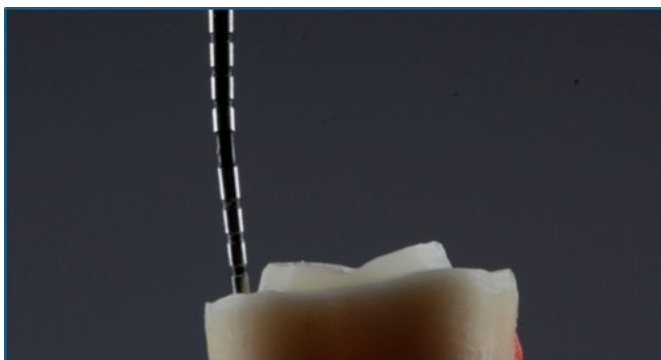


Figure 10. Proximal walls maintained at 1.0 mm confirmed radiographically



Figure 11. Minimum 1.5 mm distance preserved from chamber to finish line

Conventional Overlay Preparation: All preparation steps were identical to the ECO group, except that the pulp chamber was filled with preheated composite (Tokuyama Palfique LX5, Japan), without leaving an internal cavity. Final anatomy, wall thicknesses (1 mm), occlusal center (at CEJ level), and 1.5 mm distance to the external finish line were maintained. A butt-joint margin was prepared in enamel to standardize all restorations. All overlays were cemented using a standardized adhesive protocol. Lithium disilicate overlays were etched with 9.5% HF gel (Bisco, USA) for 20 s, rinsed, ultrasonically cleaned, alcohol-treated, and silanized with a two-part Bis-Silane system before storage. Tooth surfaces were sandblasted, cleaned with alcohol, etched with 35% phosphoric acid (Ultradent, USA), and conditioned with Clearfil Liner Bond F (Kuraray Noritake, Japan) applied in two active layers, followed by bonding resin application. A pre-heated composite resin cement (Tokuyama Palfique® Flow LX5, 60 °C) was applied to the intaglio surface, and overlays were seated with steady pressure using Compothixo™ (Kerr, USA). Excess cement was removed after tack-curing (1–2 s/surface, 3M Elipar LED), final excess cleared with an explorer, and complete polymerization performed under DeOx® gel (Ultradent, USA) from all accessible surfaces (60 s each). Figure 12 shows steps in conditioning the intaglio surface.

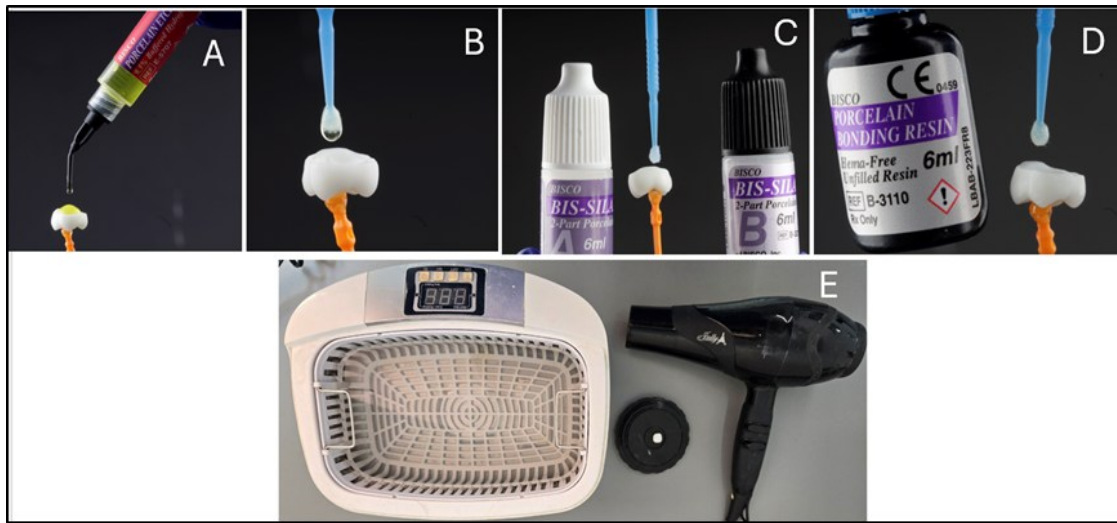


Figure 12. Steps involved in lithium disilicate conditioning. (A) Hydrofluoric acid 9.5% (Bisco, USA); (B) washing and drying; (C) two-bottle silane system (Bisco, USA); (D) non-filled ceramic bonding agent (Bisco, USA); (E) Ultrasonic water bath, air dryer, and veneer-me set used in the conditioning of the intaglio surface of the overlay

Fracture resistance test: fracture resistance was tested using a universal testing machine (Gotech Universal Testing Machine, Model U-27, Gotech Testing Machines Co., Ltd., Taiwan) A 5 mm diameter stainless-steel ball was placed in the central fossa of each overlay as shown in Figure 13. To reduce localized stress concentration and ensure even load distribution, a 0.25 mm-thick tinfoil sheet was interposed between the loading sphere and the occlusal surface, as shown in Figure 14.



Figure 13. Fracture resistance testing machine

A vertical compressive force was applied perpendicularly to the occlusal plane using a universal testing machine, operating at a crosshead speed of 0.5 mm/min, and loading continued from 0 N up to specimen fracture. The peak fracture load, expressed in Newtons (N), was defined as the highest force recorded immediately prior to a sharp

drop on the load–displacement curve. Following fracture, each specimen was inspected under $\times 20$ magnification and categorized according to failure pattern: Class I (crack confined within the restoration), Class II (cohesive failure within the restorative material), Class III (adhesive separation at the tooth–restoration interface), or Class IV (longitudinal fracture extending through both the restoration and the tooth structure).²¹



Figure 14. Tinfoil placed between loading ball and sample

Statistical Analysis

Descriptive statistics including the mean, standard deviation, minimum, and maximum values—of fracture resistance (in Newtons) were computed for each of the two experimental groups. Boxplots were generated to visually depict the distribution

of fracture resistance values according to overlay design (conventional vs. ECO overlay). To assess the suitability for parametric testing, Shapiro–Wilk tests were performed to evaluate data normality within each group. All resulting p-values exceeded 0.05, indicating no significant deviation from normality and confirming the appropriateness of parametric analysis. Independent samples t-tests were employed to compare mean fracture resistance values between two groups, with statistical significance set at $p < 0.05$. Cohen’s d effect size analysis was additionally performed to assess the magnitude of differences between groups. All statistical procedures were performed using IBM SPSS

Statistics software (Version 25.0; IBM Corp., Armonk, NY, USA).

RESULTS

Fracture resistance testing was conducted on both conventional and ECO lithium disilicate overlay groups to assess their structural integrity. Descriptive statistics for each group are summarized in Table 2. The ECO lithium disilicate overlays exhibited a significantly greater mean fracture resistance ($M = 3970.63$ N, $SD = 19.90$) than the conventional lithium disilicate overlays ($M = 2641.25$ N, $SD = 20.31$), indicating enhanced mechanical performance

Table 2. Descriptive Statistics of Fracture Resistance for Lithium Disilicate Overlays

Group	n	Mean (N)	Std. Deviation	Std. Error Mean	Min	Max
Conventional lithium disilicate overlay	8	2641.25	20.31	7.18	2615	2675
ECO lithium disilicate overlay	8	3970.63	19.90	7.04	3945	4000

An independent samples t-test confirmed a statistically significant difference between the two groups, $t(14) = 132.238$, $p < 0.001$. Cohen’s d analysis demonstrated an extremely large effect size between the groups ($d = 66.1$), indicating that

the ECO design substantially outperformed the conventional design in load-bearing capacity. The results are summarized in Table 3 and illustrated in Figure 15.

Table 3. Independent Samples t-Test – Load-to-Failure Comparison for Lithium Disilicate Overlays

Assumption	F	Sig. (Levene’s)	t	df	Sig. (2-tailed)	Mean Diff.	Std. Error Diff.	95% CI Lower	95% CI Upper
Equal variances assumed	0.008	0.930	132.238	14	0.000	1329.38	10.05	1307.81	1350.94

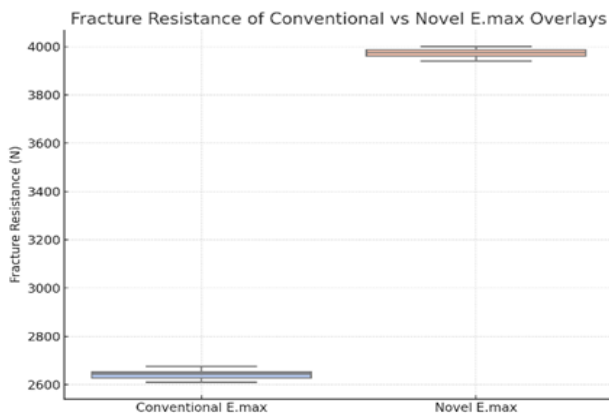


Figure 15. Boxplot of fracture resistance for conventional and ECO overlays

All specimens exhibited Type IV catastrophic fractures, characterized by deep root-involving cracks or complete structural separation. This fracture mode was likely a result of the high compressive load applied during testing. The distribution of failure modes among the experimental groups is summarized in Table 4.

Table 4. Distribution of Failure Modes Among Experimental Groups

Group	n	Class IV
Conventional lithium disilicate	8	8 (100%)
ECO lithium disilicate	8	8 (100%)

DISCUSSION

The biomechanical behavior of restored endodontically treated teeth is strongly influenced by the interaction between restorative material properties and stress distribution within the remaining tooth structure. In the present study, the incorporation of (ECO) significantly enhanced the fracture resistance of conventional lithium disilicate restorations. The enhanced performance of lithium disilicate overlays with the chambered design can be attributed to the combination of high compressive strength (~950–1200 MPa), flexural strength (~360–400 MPa), and elastic modulus (~95–105 GPa) of the material. These properties make lithium disilicate well-suited for withstanding occlusal forces, especially when stress distribution is optimized. The chambered design, by incorporating an internal air-filled cavity, appears to act as a biomechanical buffer. This allows localized vertical deformation of the dentin-cement interface under compressive load, reducing the tensile stress transmitted to the brittle ceramic restoration and minimizing crack propagation—a common failure mechanism in ceramics.^{22,23} These findings align with recent studies that have reported superior fracture resistance of lithium disilicate endocrowns and overlays, particularly when extended into or supported by the pulp chamber. Al Fodeh et al. (2023) demonstrated that lithium disilicate endocrowns outperformed zirconia overlays in both fracture load and reliability.²⁴ Similarly, Comba et al. (2022) showed that lithium disilicate outperformed polymer-infiltrated ceramics across different preparation designs under fatigue testing.²⁵ Because the ECO design partially extends into the pulp chamber space, certain biomechanical similarities with endocrown restorations may exist. Previous endocrown studies have also reported favorable fracture resistance values when utilizing pulp chamber extension for macro-retention and stress distribution.^{15,16} The relatively high fracture resistance observed in the cham-

bered lithium disilicate group in the present study may therefore be consistent with the biomechanical principles proposed for endocrown-supported restorations. An additional finding in this study was that all specimens across all groups failed through catastrophic Type IV fractures, involving root-level structural separation. This finding aligns with previous *in vitro* studies utilizing static load-to-fracture testing, in which the applied compressive forces frequently surpass normal physiologic masticatory loads, leading to irreparable failure patterns irrespective of the type of restorative material used.²¹ The present study evaluated fracture resistance under static compressive loading conditions only. However, clinical restorations are subjected to cyclic fatigue, thermal fluctuations, and multidirectional occlusal loading patterns that cannot be fully replicated by static testing alone. Therefore, the absence of thermocycling, fatigue loading, and long-term artificial aging protocols represents an important limitation of the present investigation. Future studies are recommended to evaluate the ECO design with alternative restorative materials using fatigue loading, aging protocols, and finite element analysis.

CONCLUSION

The incorporation of (ECO) in combination with lithium disilicate significantly enhanced the fracture resistance of endodontically treated mandibular molars. However, the relatively small sample size and the use of static load-to-fracture testing without fatigue aging may limit the direct clinical generalizability of the findings.

Conflict of Interest

The authors declare no conflicts of interest.

Funding

This research received no specific grant from any funding agency in the public, commercial, or not-for-profit sectors.

REFERENCES

1. Howe CA, McKendry DJ. Effect of endodontic access preparation on resistance to crown-root fracture. *J Am Dent Assoc.* 1990 Dec;121(6):712–5. doi:10.14219/jada.archive.1990.0280
2. Faria ACL, Rodrigues RCS, de Almeida Antunes RP, de Mattos M da GC, Ribeiro RF. Endodontically treated teeth: characteristics and considerations to restore them. *J Prosthodont Res.* 2011 Apr;55(2):69–74. doi:10.1016/j.jpor.2010.07.003.
3. Tang W, Wu Y, Smales RJ. Identifying and reducing risks for

- potential fractures in endodontically treated teeth. *J Endod.* 2010 Apr;36(4):609–17. doi:10.1016/j.joen.2009.12.002.
4. Soares CJ, Valdivia ADCM, da Silva GR, Santana FR, Menezes M de S. Longitudinal clinical evaluation of post systems: a literature review. *Braz Dent J.* 2012;23(2):135–40. doi:10.1590/S0103-64402012000200015.
 5. Zhu Z, Dong XY, He S, Pan X, Tang L. Effect of Post Placement on the Restoration of Endodontically Treated Teeth: A Systematic Review. *Int J Prosthodont.* 2015;28(5):475–83. doi:10.11607/ijp.4120
 6. Sarkis-Onofre R, Jacinto R de C, Boscato N, Cenci MS, Pereira-Cenci T. Cast metal vs. glass fibre posts: a randomized controlled trial with up to 3 years of follow up. *J Dent.* 2014 May;42(5):582–7. doi:10.1016/j.jdent.2014.02.003.
 7. Tezvergil A, Lassila LVJ, Vallittu PK. Strength of adhesive-bonded fiber-reinforced composites to enamel and dentin substrates. *J Adhes Dent.* 2003;5(4):301–11.
 8. Al-Zordk W, Saudi A, Abdelkader A, Taher M, Ghazy M. Fracture Resistance and Failure Mode of Mandibular Molar Restored by Occlusal Veneer: Effect of Material Type and Dental Bonding Surface. *Materials.* 2021 Oct 28;14(21):6476. doi:10.3390/ma14216476.
 9. Zarow M, Vadini M, Chojnacka-Brozek A, Szczeklik K, Milewski G, Biferi V, et al. Effect of Fiber Posts on Stress Distribution of Endodontically Treated Upper Premolars: Finite Element Analysis. *Nanomaterials.* 2020 Aug 29;10(9):1708. doi:10.3390/nano10091708.
 10. Lin CL, Chang YH, Pai CA. Evaluation of failure risks in ceramic restorations for endodontically treated premolar with MOD preparation. *Dent Mater.* 2011 May;27(5):431–8. doi:10.1016/j.dental.2010.10.026.
 11. Lin CL, Chang YH, Chang CY, Pai CA, Huang SF. Finite element and Weibull analyses to estimate failure risks in the ceramic endocrown and classical crown for endodontically treated maxillary premolar. *Eur J Oral Sci.* 2010 Feb;118(1):87–93. doi:10.1111/j.1600-0722.2009.00714.x.
 12. Magne P, Knezevic A. Simulated fatigue resistance of composite resin versus porcelain CAD/CAM overlay restorations on endodontically treated molars. *Quintessence Int.* 2009;40(2):125–33.
 13. Alshiddi IF, Aljinbaz A. Fracture resistance of endodontically treated teeth restored with indirect composite inlay and onlay restorations - An in vitro study. *Saudi Dent J.* 2016 Jan;28(1):49–55. doi:10.1016/j.sdentj.2015.11.001.
 14. Zhu J, Rong Q, Wang X, Gao X. Influence of remaining tooth structure and restorative material type on stress distribution in endodontically treated maxillary premolars: A finite element analysis. *J Prosthet Dent.* 2017 May;117(5):646–55. doi:10.1016/j.prosdent.2016.08.019.
 15. Pissis P. Fabrication of a metal-free ceramic restoration utilizing the monobloc technique. *Pract Periodontics Aesthet Dent.* 1995;7:83–94.
 16. Bindl A, Mörmann W. Clinical evaluation of adhesively placed Cerec endo-crowns after 2 years: Preliminary results. *J Adhes Dent.* 1999;1:255–65.
 17. Magne P. Efficient 3D finite element analysis of dental restorative procedures using micro-CT data. *Dent Mater.* 2007 May;23(5):539–48. doi:10.1016/j.dental.2006.03.013.
 18. Fasbinder D. Using digital technology to enhance restorative dentistry. *Compend Contin Educ Dent Jamesburg NJ* 1995. 2012 Oct;33(9):666–8, 670, 672 passim.
 19. Fasbinder DJ. Digital dentistry: innovation for restorative treatment. *Compend Contin Educ Dent Jamesburg NJ* 1995. 2010;31 Spec No 4:2–11; quiz 12.
 20. Tsatsoulis IN, Filippatos CG, Floratos SG, Kontakiotis EG. Estimation of radiographic angles and distances in coronal part of mandibular molars: A study of panoramic radiographs using EMAGO software. *Eur J Dent.* 2014 Jan;8(1):90–4. doi:10.4103/1305-7456.126257.
 21. Guess PC, Schultheis S, Wolkewitz M, Zhang Y, Strub JR. Influence of preparation design and ceramic thicknesses on fracture resistance and failure modes of premolar partial coverage restorations. *J Prosthet Dent.* 2013 Oct 1;110(4):264–73. doi:10.1016/S0022-3913(13)60347-2.
 22. Kelly JR, Benetti P. Ceramic materials in dentistry: historical evolution and current practice. *Aust Dent J.* 2011 Jun;56 Suppl 1:84–96. doi:10.1111/j.1834-7819.2010.01299.x
 23. Kinney JH, Marshall SJ, Marshall GW. The mechanical properties of human dentin: a critical review and re-evaluation of the dental literature. *Crit Rev Oral Biol Med.* 2003;14(1):13–29. doi:10.1177/154411130301400103.
 24. Al Fodeh RS, Al-Johi OS, Alibrahim AN, Al-Dwairi ZN, Al-Haj Husain N, Özcan M. Fracture strength of endocrown maxillary restorations using different preparation designs and materials. *J Mech Behav Biomed Mater.* 2023 Dec 1;148:106184. doi:10.1016/j.jmbbm.2023.106184.
 25. Comba A, Baldi A, Carossa M, Michelotto Tempesta R, Garino E, Llubani X, et al. Post-Fatigue Fracture Resistance of Lithium Disilicate and Polymer-Infiltrated Ceramic Network Indirect Restorations over Endodontically-Treated Molars with Different Preparation Designs: An In-Vitro Study. *Polymers.* 2022 Nov 23;14(23):5084. doi:10.3390/polym14235084.